

Nitrogen-Rich Perylene Nanosheet Enhanced Bismaleimide Resin

Yuting Peng¹, Yan Luo¹, Qian Wu¹, Yun Huang² and Long Yang^{1,*}

¹State Key Laboratory of Environment-Friendly Energy Materials, School of Materials Science and Chemistry, Southwest University of Science and Technology, Mianyang 621010, Sichuan, China

²State Key Laboratory of Polymer Materials Engineering of China (Sichuan University), Polymer Research Institute of Sichuan University, Chengdu 610065, China

Abstract: The low toughness of bismaleimide resin (BMI) hinders its application in the aerospace field. In order to improve the strength and toughness of BMI resin simultaneously, this study proposes to introduce perylene-dicyandiamide (P-DCD) nanosheets with an ultra-s rigid conjugated planar structure into the polymer matrix of bismaleimide resin through hydrogen bonding and cross-linking to construct modified composites. The research results showed that the modified cured composites exhibited excellent mechanical properties, with a significant increase in impact strength of 135.8%, flexural strength and flexural modulus of 87.1% and 44.6%, respectively. The thermal properties of the resin were maintained before and after modification, with the glass transition temperature (T_g) of 284.0 °C and decomposition temperature > 520 °C. Meanwhile, the strengthening and toughening mechanism of the bismaleimide-based system modified by additive P-DCD were also explored. The results showed that the functional group of dicyandiamide in nanosheets and the hydrogen bonding effect in P-DCD synergistically increased the cross-linking network and compatibility between P-DCD and the matrix resin.

Keywords: Bismaleimides (BMI), Composite Material, Toughening, Mechanical Property, Thermal Property.

1. INTRODUCTION

Due to its high strength and stability, advanced composite materials are widely used in various fields such as the electronics industry and aerospace. Polyimides are thermos-resistant polymers with imide groups in the main chain, which have been intensively studied since the 1960s for their excellent thermal stability and high mechanical properties, along with their super chemical resistance and electrical properties [1,2]. As a matrix of fiber reinforced plastics or composites, Bismaleimide (BMI) is a new type of thermosetting resin derived from the imide resin system in polyimide-based advanced composites, which not only retains the advantages of high-temperature resistance of polyimide resin, but also have excellent processability, corrosion resistance, low shrinkage, and low creep properties comparable to epoxy resin. Because of its high chemical stability, excellent thermal resistance, good radiation resistance, and low water absorption, it can be used for a long time at 170 °C in a wet environment, and after post-curing treatment, its dry state use temperature can even reach 230 °C~250 °C, [3-5] and it is widely applied in many related industries such as aerospace and electronics industry [6-8]. Additionally, the pristine BMI resin exhibits easy process ability similar to the epoxy resin so the cost of manufacturing was low. However, the conventional BMI resin still has drawbacks such as high brittleness, poor

impact resistance, and crack resistance caused by high cross-linking density [9-12]. Therefore, in practical applications, it is crucial to toughen BMI resin while ensuring its excellent inherent properties to support it from significant deformation under high stress. Much research has focused on modifying BMI resin to improve its toughness [13-15].

From a supramolecular and material point of view, coplanarity and rigidity often promote strong intermolecular electronic coupling and reduce the energy barrier for the intermolecular transport of charges, excitons, and phonons, affording advanced materials properties in bulk [16]. Therefore, Perylene-Dicyandiamide (P-DCD) nanosheets can be an ideal filler for advanced composite materials, because of its ultra-s rigid conjugated planar structure [17]. Ma [18] introduced a rigid planar 2,5-diphenyl-[1,3,4]-oxadiazole structure with strong intermolecular π - π stacking interactions into the main chain of resins, the corresponding cured resins had high mechanical properties and relaxation temperature. Ding [19] fabricated a modified conjugated molecule curing agent Ethyl Glycidyl Ether-2-Methylimidazole (EGE-2-MI). The epoxy resin system using EGE-2-MI as the curing agent can be efficiently cured at 110-120 °C. This novel moderate-temperature curing system with decent storage life and mechanical properties can overcome the rooted disadvantage of imidazole curing agents.

In this work, we synthesized a new 2D material (P-DCD) based on hydrogen bonding with a large π -conjugated system and nitrogen-rich atoms and used it

*Address corresponding to this author at the State Key Laboratory of Environment-Friendly Energy Materials, School of Materials Science and Chemistry, Southwest University of Science and Technology, Mianyang 621010, Sichuan, China; E-mail: yanglong@swust.edu.cn

as the modified curing agent. P-DCD not only introduced hydrogen bonds, but also changed the cross-linking structure of BMI resin to obtain composite materials with excellent mechanical properties, which provides a promising approach for developing high-performance BMI composite materials.

2. EXPERIMENTAL

2.1. Materials

4,4'-Bismaleimidodiphenyl methane (BMI), dicyandiamine (DCD), and N,N-dimethyl formamide was purchased from Shanghai Macklin Biochemical Technology (Shanghai, China) Co., Ltd. BMI was commercial grade yellow powder containing more than 85% of maleimide double-bond structure. Perylene-3,4,9,10-tetracarboxylic dianhydride (PTCDA) was provided by Shanghai Aladdin Biochemical Technology (Shanghai, China) Co., Ltd. 4,4'-(4,4'-Isopropylidenediphenyl-1,1'-Diyldioxy) Dianiline was received from Shanghai Taitan Scientific Co., Ltd. Ethylene glycol, dichloromethane, acetone and anhydrous methanol were supplied from Chengdu Chron chemical (Chengdu, China) Co., Ltd.

2.2. Synthesis of P-DCD

First, PTCDA (2 g, 5.098 mmol) and DCD (4 g, 47.574 mmol) were dissolved in 40 mL N,N-dimethyl formamide and 40 mL ethylene glycol solvent, mixed homogeneously, and then fully reacted in the solvent at 200 °C for 60 h. After the reaction was completed, the red solution product was washed several times with a large amount of anhydrous alcohol, dichloromethane,

acetone, N,N-dimethyl formamide, and deionized water sequentially to remove the residual reactant. Finally, the samples were freeze dried at -60 °C for 12 h in a vacuum to obtain Perylene-Dicyandiamide (P-DCD) organic nanosheets containing ultra-rigid conjugated planar structure.

2.3. Synthesis of Dianiline+P-DCD/BMI Resins

Dianiline+P-DCD/BMI thermosets fabricated with various weight ratios of as-synthesized Dianiline, P-DCD and BMI matrix. Firstly, different amounts of P-DCD and dianiline were added to the above BMI and milled and blended uniformly to get the copolymer (donated as X-Dianiline+Y-P-DCD/BMI, where X represents the mass fraction of Dianiline and Y represents the mass fraction of P-DCD).

Afterward, the copolymer was poured into a PTFE mold and cured following the procedures of 100 °C/1h + 180 °C/3h + 200 °C/2h + 260 °C/2h. Finally, the modified P-DCD+Dianiline /BMI resin was cooled down to room temperature and demolded for further testing.

2.4. Characterizations

Structural characterization of P-DCD and resins was studied by X-ray diffraction (XRD) patterns, which were recorded on an X'Pert PRO diffractometer using a Ceramic Cu X-ray tube at a scanning rate of 5°/min⁻¹ between 5° and 60°. Solid-state ¹³C CP/MAS NMR spectroscopy was carried out on a Bruker Avance III TM 600 MHz NMR spectrometer. Fourier transform infrared spectra (FT-IR) were recorded in the region 400 to 4000 cm⁻¹ on a Nicolet-5700 spectrometer.

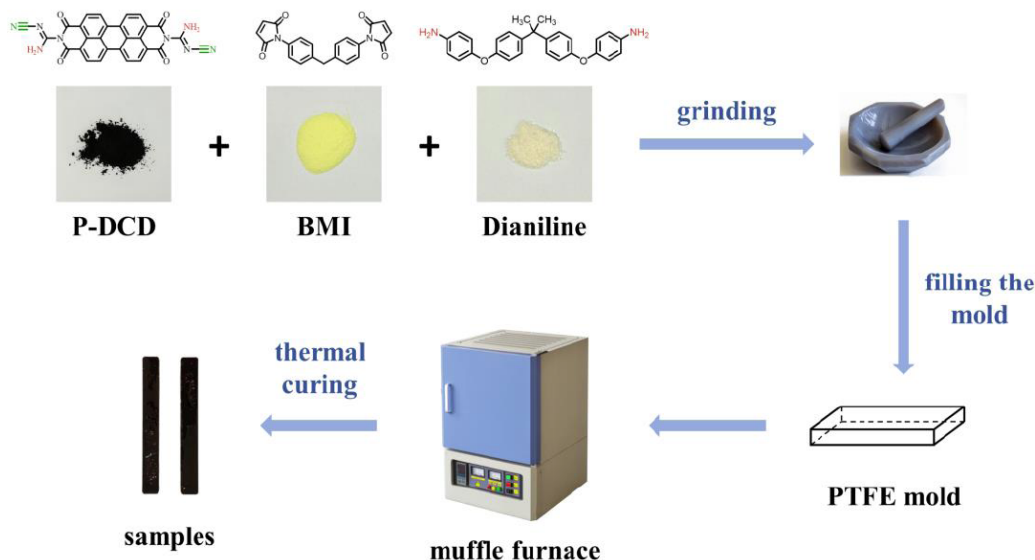


Figure 1: Synthesis process diagram of Dianiline+P-DCD/BMI resins

(U.S.A) with a resolution of 0.5 cm^{-1} . Differential scanning calorimetry (DSC, PE DSC6000, U.S.A) was used to determine the curing property by isothermal ($10\text{ K}\cdot\text{min}^{-1}$) from $50\text{ }^{\circ}\text{C}$ to $380\text{ }^{\circ}\text{C}$ under N_2 atmosphere. The different composite materials were tanked into a DSC aluminum crucible. The morphology of P-DCD was observed by Scanning Electron Microscope (SEM, Ultra55, Germany). The morphology and high-resolution lattice of P-DCD were conducted by transmission electron microscope (TEM, FEI Talos 200X, U.S.A). The impact strength was carried out according to GB/T 1843-2008 (Chinese standard) and measured by an impact testing machine (JJ-15) with the sample dimension of $80\text{ mm} \times 10\text{ mm} \times 4\text{ mm}^3$. The flexural strength and flexural modulus were carried out according to GB/T 9341-2008 (Chinese standard) and measured by an electronic universal testing machine (WSM-30KN) with the crosshead speed set at 2 mm min^{-1} .

3. RESULTS AND DISCUSSION

3.1. Structural Characterization of P-DCD

The XRD pattern of P-DCD nanosheets is shown in Figure 2a, with a distinct π - π stacking peak at $2\theta = 27.2^{\circ}$ corresponding to its lattice spacing of 3.28 \AA . Nitrogen-rich group stacking (3.54 \AA and 7.73 \AA). Which demonstrated the successful synthesis of the additive P-DCD. Meanwhile, the XRD pattern of P-DCD displayed high absorption intensity, suggesting that the product synthesized herein has a crystal structure and

high purity, proving its crystalline and aggregated state structural features.

The solid-state ^{13}C NMR spectrum (Figure 2b) was presented to further verify the chemical structure of P-DCD. In Figure 2b, the peaks at 120 to 131 ppm are assigned to the characteristic peaks of the perylene part. The signal at 161 ppm is observed for $-\text{C}=\text{O}$ group part. The signal located at 164 ppm is attributed to the nitrogen-rich part [20]. According to the above considerate analysis, the results demonstrate that the target product P-DCD was successfully synthesized.

The FT-IR spectra of DCD, PTCDA, and P-DCD were presented in Figure 2c. The absorption peaks at 2207 cm^{-1} and 1639 cm^{-1} are attributed to stretching vibrations of $\text{C}\equiv\text{N}$ and $\text{C}=\text{N}$ in the spectrum of DCD. The characteristic peaks of PTCDA are separately detected at 1772 cm^{-1} for $\text{C}=\text{O}$ bonds, 1594 cm^{-1} for $\text{C}=\text{C}$ bonds, and 1022 cm^{-1} for $\text{C}-\text{O}$. In comparison with DCD, the stretching vibration peak of $\text{N}-\text{H}$ bonds at 3121 cm^{-1} moves to the higher wave number, which is caused by the appearance of hydrogen bonding. In the spectrum of P-DCD, the peak corresponding to carbonyl ($\text{C}=\text{O}$) stretching vibration, initially positioned at 1772 cm^{-1} , changed to 1689 cm^{-1} due to full imidization [21-24]. This spectral signature suggested the disappearance of anhydride ($\text{O}=\text{C}-\text{O}-\text{C}=\text{O}$) group and the complete imidization between anhydride ($\text{O}=\text{C}-\text{O}-\text{C}=\text{O}$) and amine ($-\text{NH}_2$) groups in PTCDA and DCD, respectively. In addition, the slight blue shift in the perylene-ring skeleton vibration peak ($\text{C}=\text{C}$, from

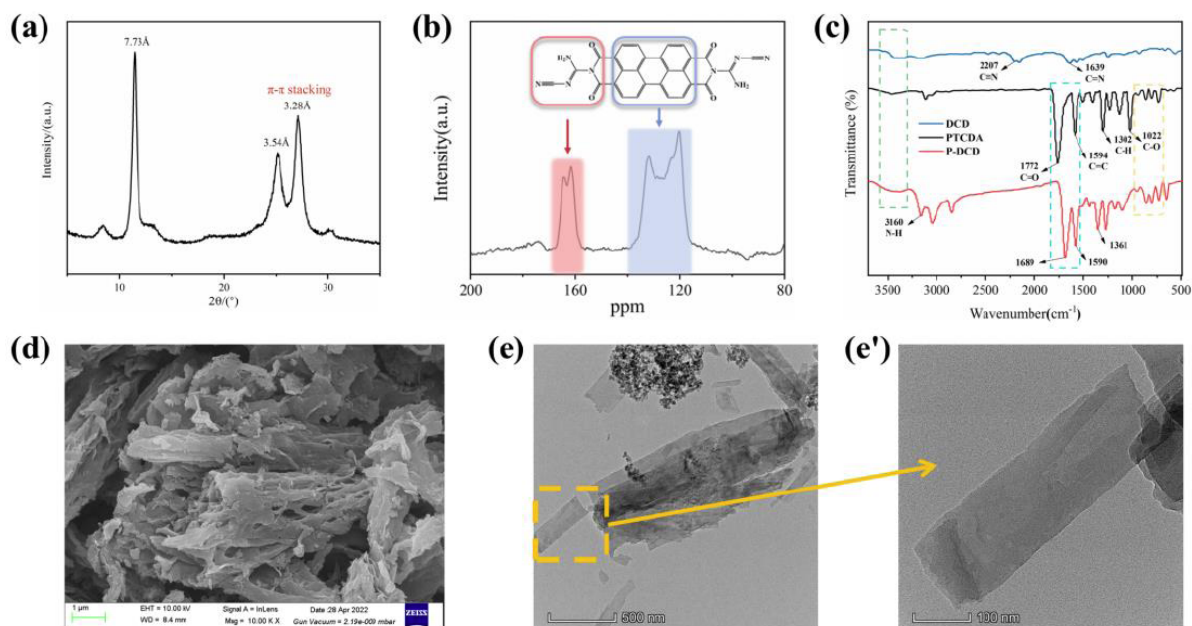


Figure 2: Structural characterizations of P-DCD. (a) XRD patterns, (b) ^{13}C NMR spectra, (c) FT-IR spectrum, (d) SEM image, (e) and (e') TEM images

1594 cm^{-1} to 1590 cm^{-1}) indicated the enhanced π - π stacking [25-27]. Compared with PTCDA, the peak corresponding to the bending vibration of C-H changes from 1302 cm^{-1} to 1361 cm^{-1} , the characteristic peak C-O (1022 cm^{-1}) of PTCDA is weakened, and the four peaks at 950-730 cm^{-1} represent the stretching vibration of C-N and the bending vibration of C-H and N-H.

SEM and TEM images of P-DCD are shown in Figure 2d~e'. It clearly showed that P-DCD formed a regular nanosheet morphology. The above characterization confirmed that P-DCD was successfully synthesized.

3.2. Curing Behavior of Dianiline+P-DCD/BMI Resins

In order to study the changes of chemical structure during the curing process, FT-IR technique was adopted to investigate the possible curing reactions of pure BMI and 0.25 Dianiline +0.1 P-DCD/BMI resin, and the FTIR spectrum is shown in Figure 3a. As shown in Figure 3a, the absorption peaks of located at 2922 cm^{-1} (C=C) and 2852 cm^{-1} (C-H) are ascribed to the ring of BMI. At 1699 cm^{-1} is the characteristic the peak of carbonyl group (-C=O) on the ring of imide, and a band related to the benzene ring at 1511 cm^{-1} . In addition, the BMI showed the absorption bands characteristic of maleimide groups at 1143, 823, and 688 cm^{-1} . The stretching vibration absorption of C-N-C

on the maleimide ring at 1143 cm^{-1} , the out-of-plane vibration absorption of the C=C double bond on the BMI ring at 823 cm^{-1} , and the characteristic absorption peak at 688 cm^{-1} is=C-H [28]. With the proceeding of curing reaction, the characteristic peaks of the N-H at 3749 and 3628 cm^{-1} , as well as C≡N characteristic peaks at 2000 cm^{-1} emerge. The C=C at 2927 cm^{-1} and the C-H absorption peak at 2852 cm^{-1} on the BMI ring show sharp absorption peaks, while the corresponding C=O, benzene ring, and C-N-C peaks at 1728, 1542, and 1178 cm^{-1} were weakened in intensity. The characteristic absorption peaks of C=C and =C-H on the maleimide groups at 823 and 688 cm^{-1} are almost disappearing. The above changes indicate that the reaction is essentially complete, suggesting that the curing process is feasible.

The reactions between Dianiline, P-DCD, and BMI resin can be further confirmed by the XRD curves of the composite resins as shown in Figure 3b. The XRD spectra of all composite resins are almost similar to the pure BMI resin. In detail, there are two peaks appearing at $2\theta=18.3^\circ$ and $2\theta=39.1^\circ$ in the diffraction pattern of BMI resin, whereas the peak at $2\theta=18.3^\circ$ gradually becomes progressively sharper and shifts toward smaller angles with increasing the content of Dianiline and P-DCD, reflecting that there is an interaction between Dianiline, P-DCD and BMI resin, and thus producing a loss of regularity with respect to pure P-DCD crystals. Moreover, the characteristic

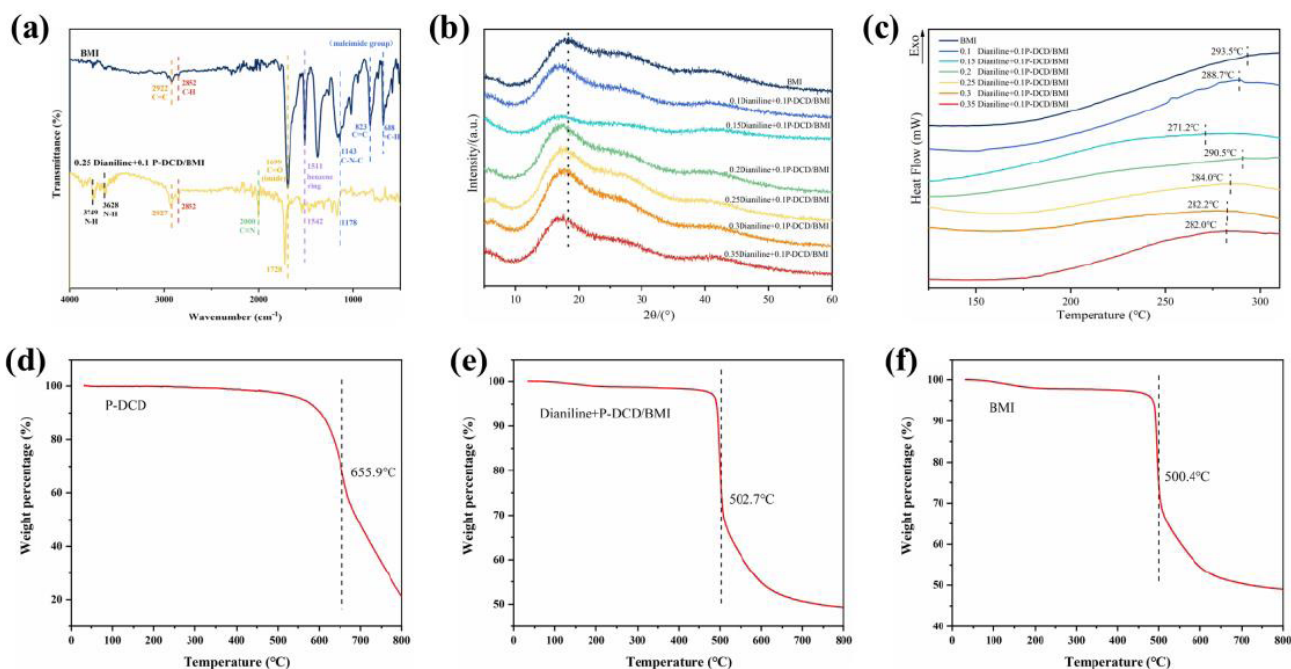


Figure 3: Characterizations of the curing behaviors BMI composite resin. (a) FT-IR spectrum, (b) XRD patterns, (c) DSC curves, (d) TGA curve of P-DCD, (e) TGA curve of Dianiline+P-DCD/BMI resin, (f) TGA curve of BMI resin.

diffraction peak of P-DCD at $2\theta=11.4^\circ$ is not observed, indicating that P-DCD is mixed with other components at a molecular level without the formation of P-DCD crystallite.

To further clarify the remarkable curing behavior of Dianiline+P-DCD/BMI resins, the DSC technique was adopted to investigate the possible curing reactions of pure BMI and Dianiline+P-DCD/BMI resins. The DSC curves are shown in Figure 3c, showing similar single exothermic peaks, which indicate that the Dianiline+P-DCD/BMI system reacts homogeneously, and the additives P-DCD and Dianiline have good compatibility with the resin matrix, as the additives contain a large amount of active terminal amino groups. Compared to the T_g value of BMI resin, the addition of dianiline and P-DCD causes T_g to transfer to a lower temperature. The slight decrease in the peak temperature of the 0.15 P-DCD/BMI resins from 293.5°C to 271.2°C as compared to the pure BMI is due to the changes in the molecular structure of the polymer induced by the introduction of the dianiline and P-DCD. This may be due to the production of a substance with relatively poor heat resistance, resulting in a slight decrease in the thermal stability of the composite resin. The overall T_g value of this composite resin material is relatively high, exceeding 270°C , and the high T_g ensures its application in high-temperature environments.

In addition, the TGA tests of P-DCD, composite resins, and BMI resin in Figure 3d~f show that the

decomposition temperature of the composite resins exceeds 500°C , it has increased by about 50°C compared to other literature, indicating that the modified BMI resins maintain good thermal stability. Dianiline+P-DCD/BMI showed similar thermal stability to P-DCD/BMI due to the low amount of added P-DCD and dianiline.

3.3. Mechanical Properties of Dianiline+P-DCD/BMI Resins

As can be seen from Figure 4, the addition of modified dianiline and P-DCD organic nanosheets can toughen the BMI resin, and significantly improve the impact strength, flexural strength, and flexural modulus, of which Figure 4 modified dianiline can be added according to the addition of 0.1wt%-0.35wt% can be obtained a better modification effect (when the addition amount of modified P-DCD organic nanosheets is all 0.1wt%), the most significant improvement in the mechanical properties of the composites obtained when modified P-DCD is added to the bismaleimide resin according to 0.25wt%. When 0.1wt% modified perylene dicyandiamide organic nanosheets and 0.25wt% modified dianiline were added, the impact strength of the BMI resin composite material increased by 135.8% compared to the matrix, and the flexural strength and flexural modulus were increased by 87.1% and 44.6%, respectively, compared with the pure bismaleimide resin matrix. Figure 5 shows the resin samples with different proportions, through the

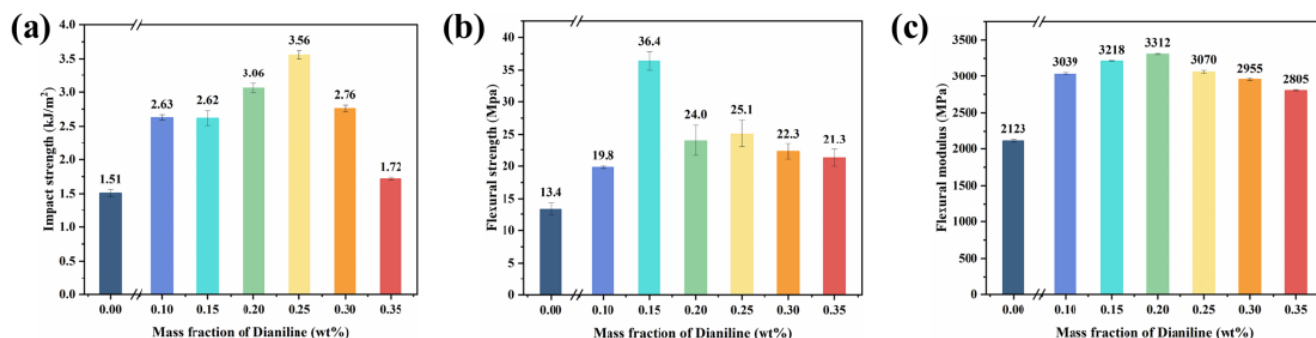


Figure 4: Impact strength (a), flexural strength (b), flexural modulus (c) on Dianiline+P-DCD/BMI resin.



Figure 5: Resin samples at different proportions. (a) 0.25 Dianiline+0.1 P-DCD/BMI, (b) 0.2 Dianiline/BMI, (c) 0.25 P-DCD/BMI.

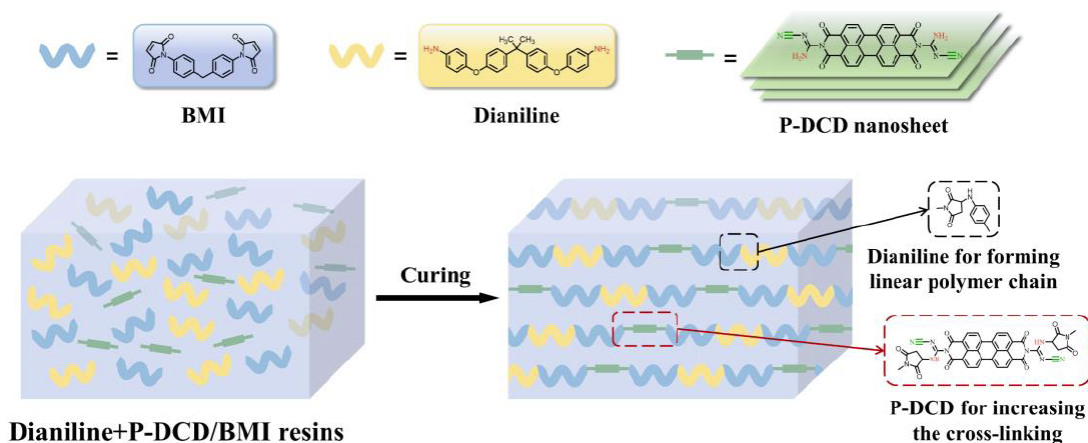


Figure 6: Schematic diagram of strengthening and toughening mechanism on BMI resins.

novel perylene-based nitrogen-rich organic nanosheets modification and the addition of a certain amount of dianiline, the mechanical properties of the modified BMI resins obtained were significantly improved, and the problems of the bismaleimide cured products showing obvious brittleness and poor fracture toughness were solved.

The schematic diagram of the strengthening and toughening mechanism is exhibited in Figure 6. Due to the dual functional groups of dianiline and BMI, a linear polymer chain without cross-linking is formed. Furthermore, due to the chemical and physical stability of P-DCD nanosheets, which have a stacked structure and are rich in amino groups, individual P-DCD molecules are unable to cross-link BMI, but P-DCD nanosheets [29]. The addition of rigid π - π conjugated P-DCD increased the cross-linking of the polymer chains, the terminated amino groups of P-DCD acted as cross-linked points to generate a tight interface bonding, maintaining the structural integrity of the polymer matrix for strengthening [30-31]. Additionally, redundant dianiline addition tends to accelerate the local excessive cross-linking of modified resins leading to deteriorated mechanical properties of the resin matrix.

4. CONCLUSIONS

In general, novel Perylene-Dicyandiamide (P-DCD) nanosheets with an ultra-rigid conjugated planar structure were synthesized and introduced into the polymer matrix of bismaleimide resin through hydrogen bonding and cross-linking to achieve excellent mechanical performance and desirable thermal performance. The results showed that the functional group dicyandiamide nanosheets and the hydrogen bonding effect in P-DCD increased the compatibility

between P-DCD and the matrix resin. P-DCD not only introduced hydrogen bonds, but also changed the cross-linking structure of BMI resin to obtain composite materials with excellent mechanical properties, which provides a promising approach for developing high-performance BMI composite materials.

ACKNOWLEDGEMENT

The authors are grateful to the Natural Science Foundation of Sichuan Province (No. 2022 NSFSC0195) and the National Natural Science Foundation of China (No. 22102134).

REFERENCE

- [1] Patel YS, Patel HS. Thermoplastic-Thermosetting Merged Polyimides Derived from Furan-Maleimide [J]. Journal of Research Updates in Polymer Science 2012; (1): 75-83. <https://doi.org/10.6000/1929-5995.2012.01.02.3>
- [2] Horacek H. Mono- and Bis- Maleimide Resins in Preimpregnated Fibres [J]. Journal of Research Updates in Polymer Science 2020; (9): 1-23. <https://doi.org/10.6000/1929-5995.2020.09.01>
- [3] Iredale RJ, Ward C, Hamerton I. Modern Advances in Bismaleimide Resin Technology: A 21st Century Perspective on the Chemistry of Addition Polyimides[J]. Progress in Polymer Science 2017; (69): 1-21. <https://doi.org/10.1016/j.progpolymsci.2016.12.002>
- [4] Chandra R, Rajabi L. Recent Advances in Bismaleimides and Epoxy-Imide/ Bismaleimide Formulations and Composites[J]. Journal of Macromolecular Science Part C 1997; 37(1): 61-96. <https://doi.org/10.1080/15321799708014733>
- [5] Zou Q, Xiao F, Gu SQ, et al. Toughening of Bismaleimide Resin Based on Self-Assembly of Flexible Aliphatic Side Chains[J]. Industrial & Engineering Chemistry Research 2019; 58(36): 16526-16531. <https://doi.org/10.1021/acs.iecr.9b01822>
- [6] Robertson FC. Resin Transfer Moulding of Aerospace Resins-A Review [J]. British Polymer Journal 1988; (20): 417-429. <https://doi.org/10.1002/pi.4980200506>
- [7] White JE. Synthesis and Properties of High-Molecular-Weight Step-Growth Polymers from Bismaleimides[J]. Industrial & Engineering Chemistry Product Research & Development 1986; 25(3): 395-400. <https://doi.org/10.1021/i300023a005>

- [8] Konarski MM. Development of a Toughened Bismaleimide Resin Matrix for use in Advanced Composites [J]. High Performance Polymers 1989; 1(4): 299-310.
<https://doi.org/10.1177/095400838900100404>
- [9] Liu C, Qiao Y, Li N, *et al.* Toughened of Bismaleimide Resin with Improved Thermal Properties using Amino-Terminated Poly(phthalazinone ether nitrile sulfone)s[J]. Polymer 2020; (206): 122887.
<https://doi.org/10.1016/j.polymer.2020.122887>
- [10] Melissaris AP, Mikroyannidis JA. Thermally S Polymers Based on Bismaleimides Containing Amide, Imide, and Ester Linkages[J]. Journal of Polymer Science Part A: Polymer Chemistry 1989; 27(1): 245-262.
<https://doi.org/10.1002/pola.1989.080270121>
- [11] Krishnadevi K, Selvaraj V, Prasanna D. Thermal, Mechanical and Antibacterial Properties of Cyclophosphazene Incorporated Benzoxazine Blended Bismaleimide Composites[J]. RSC Advances 2015; 5(2): 913-921.
<https://doi.org/10.1039/C4RA10564H>
- [12] Rao V, Navath S, Kottur M, *et al.* An Efficient Reverse Diels–Alder Approach for the Synthesis of N-alkyl Bismaleimides[J]. Tetrahedron Letters 2013; (54): 5011-5013.
<https://doi.org/10.1016/j.tetlet.2013.07.002>
- [13] Xia L, Xu Y, Wang K, *et al.* Preparation and Properties of Modified Bismaleimide Resins by Novel Bismaleimide Containing 1,3,4-oxadiazole[J]. Polymers for Advanced Technologies 2015; 26(3): 266-276.
<https://doi.org/10.1002/pat.3452>
- [14] Wang X, Jiang Q, Xu W, *et al.* Effect of Carbon Nanotube Length on Thermal, Electrical and Mechanical Properties of CNT/Bismaleimide Composites [J]. Carbon 2013; (53): 145-152.
<https://doi.org/10.1016/j.carbon.2012.10.041>
- [15] Zhao L, Liu P, Liang G, *et al.* The Origin of the Curing Behavior, Mechanical and Thermal Properties of Surface Functionalized Attapulgite/Bismaleimide/Diallylbisphenol Composites [J]. Applied Surface Science 2014; (288): 435-443.
<https://doi.org/10.1016/j.apsusc.2013.10.052>
- [16] Zhu C, Kalin AJ, Fang L. Covalent and Noncovalent Approaches to Rigid Coplanar π -Conjugated Molecules and Macromolecules [J]. Accounts of Chemical Research 2019; 52(4): 1089-1100.
<https://doi.org/10.1021/acs.accounts.9b00022>
- [17] Yang L, Peng Y, Luo X, *et al.* Beyond C_3N_4 π -Conjugated Metal-Free Polymeric Semiconductors for Photocatalytic Chemical Transformations[J]. Chemical Society Reviews 2021; 50(3): 2147-2172.
<https://doi.org/10.1039/D0CS00445F>
- [18] Ma M, Gong C, Li C. *et al.* The Synthesis and Properties of Silicon-Containing Arylacetylene Resins with Rigid-Rod 2,5-diphenyl-[1,3,4]-oxadiazole moieties [J]. European Polymer Journal 2021; 143(1): 110192.
<https://doi.org/10.1016/j.eurpolymj.2020.110192>
- [19] Ding L, Yang JP, Hao XL, *et al.* Fabrication and Characterization of a Modified Conjugated Molecule-Based Moderate-Temperature Curing Epoxy Resin System[J]. Frontiers in Materials 2020; (7): 577-962.
<https://doi.org/10.3389/fmats.2020.577962>
- [20] Zhang H, Chen X, Zhang Z, *et al.* Highly-Crystalline Triazine-PDI Polymer with an Enhanced Built-in Electric Field for Full-Spectrum Photocatalytic Phenol Mineralization [J]. Applied Catalysis B: Environmental 2021; (287): 119957.
<https://doi.org/10.1016/j.apcatb.2021.119957>
- [21] Zhang K, Wang J, Jiang W, *et al.* Self-Assembled Perylene Diimide Based Supramolecular Heterojunction with Bi_2WO_6 for Efficient Visible-Light-Driven Photocatalysis [J]. Applied Catalysis B: Environmental 2018; (232): 175-181.
<https://doi.org/10.1016/j.apcatb.2018.03.059>
- [22] Dai W, Jiang L, Wang J, *et al.* Efficient and S Photocatalytic Degradation of Tetracycline Wastewater by 3D Polyaniline/Perylene Diimide Organic Heterojunction under Visible Light Irradiation [J]. Chemical Engineering Journal 2020; (397): 125476.
<https://doi.org/10.1016/j.cej.2020.125476>
- [23] Kong K, Zhang S, Chu Y. *et al.* A Self-Assembled Perylene Diimide Nanobelt for Efficient Visible-Light-Driven Photocatalytic H_2 Evolution [J]. Chemical Communications 2019; (55): 8090-8093.
<https://doi.org/10.1039/C9CC03465J>
- [24] Xie Y, Ye M, Xiong B, *et al.* Enhanced Reactive-Oxygen-Species Generation and Photocatalytic Efficiency with Internal Imide Structures of Different Ratio in Metal-Free Perylene-g- C_3N_4 Semiconductors [J]. Applied Surface Science 2021; (546): 149138.
<https://doi.org/10.1016/j.apsusc.2021.149138>
- [25] Yang J, Miao H, Wei Y, *et al.* π - π Interaction Between Self-Assembled Perylene Diimide and 3D Graphene for Excellent Visible-Light Photocatalytic Activity [J]. Applied Catalysis B: Environmental 2019; (240): 225-233.
<https://doi.org/10.1016/j.apcatb.2018.09.003>
- [26] Sheng Y, Miao H, Jing J, *et al.* Perylene Diimide Anchored Graphene 3D Structure via π - π Interaction for Enhanced Photoelectrochemical Degradation Performances [J]. Applied Catalysis B: Environmental 2020; (272): 118-897.
<https://doi.org/10.1016/j.apcatb.2020.118897>
- [27] Angelella M, Wang C, Tauber M J. Resonance Raman Spectra of a Perylene Bis(dicarboximide) Chromophore in Ground and Lowest Triplet States[J]. Journal of Physical Chemistry A 2013; 117(38): 9196-9204.
<https://doi.org/10.1021/jp407879k>
- [28] Shibata M, Satoh K, Ehara S. Thermosetting Bismaleimide Resins Generating Covalent and Multiple Hydrogen Bonds[J]. Journal of Applied Polymer Science 2016; 133.
<https://doi.org/10.1002/app.43121>
- [29] Tang J, Yang R, Peng Y, *et al.* Ultra-Thin Hydrogen-Organic-Framework (HOF) Nanosheets for Ultra-S Alkali Ions Battery Storage[J]. Small 2023; 2307827.
<https://doi.org/10.1002/sml.202307827>
- [30] Li K, Zhou L, Wu S, *et al.* A Facile Synthesis of Soluble Polyimides with High Glass Transition Temperature and Excellent Mechanical Properties due to Intermolecular Hydrogen Bonds [J]. High Performance Polymers 2020; 32(3): 316-323.
<https://doi.org/10.1177/0954008319861141>
- [31] Li K, Yang L, He H, *et al.* Aramid-Film pH Sensitive Fluorescence Enhancement Based on Benzimidazole Intermolecular Hydrogen Bonds [J]. Optical Materials 2022; (123): 111-903.
<https://doi.org/10.1016/j.optmat.2021.111903>

Received on 2-10-2023

Accepted on 25-11-2023

Published on 21-12-2023

<https://doi.org/10.6000/1929-5995.2023.12.20>© 2023 Peng *et al.*; Licensee Lifescience Global.

This is an open-access article licensed under the terms of the Creative Commons Attribution License (<http://creativecommons.org/licenses/by/4.0/>), which permits unrestricted use, distribution, and reproduction in any medium, provided the work is properly cited.